AVAZ inversion for fracture weakness parameters based on the rock physics model

2014 J. Geophys. Eng. 11 065007

(http://iopscience.iop.org/1742-2140/11/6/065007)

IOP Publishing Journal of Geophysics and Engineering

J. Geophys. Eng. **11** (2014) 065007 (9pp) doi:10.1088/1742-2132/11/6/065007

AVAZ inversion for fracture weakness parameters based on the rock physics model

Huaizhen Chen[1], Xingyao Yin[1], Shouli Qu[2] and Guangzhi Zhang[1]

[1] School of Geosciences, China University of Petroleum, Qingdao, People's Republic of China
[2] Sinopec Geophysical Research Institute, Nanjing, People's Republic of China

E-mail: chenhz2011@gmail.com

Received 24 March 2014, revised 30 September 2014
Accepted for publication 30 September 2014
Published 6 November 2014

Abstract

Subsurface fractures within many carbonates and unconventional resources play an important role in the storage and movement of fluid. The more reliably the detection of fractures could be performed, the more finely the reservoir description could be made. In this paper, we aim to propose a method which uses two important tools, a fractured anisotropic rock physics effective model and AVAZ (amplitude versus incident and azimuthal angle) inversion, to predict fractures from azimuthal seismic data. We assume that the rock, which contains one or more sets of vertical or sub-vertical fractures, shows transverse isotropy with a horizontal axis of symmetry (HTI). Firstly, we develop one improved fractured anisotropic rock physics effective model. Using this model, we estimate P-wave velocity, S-wave velocity and fracture weaknesses from well-logging data. Then the method is proposed to predict fractures from azimuthal seismic data based on AVAZ inversion, and well A is used to verify the reliability of the improved rock physics effective model. Results show that the estimated results are consistent with the real log value, and the variation of fracture weaknesses may detect the locations of fractures. The damped least squares method, which uses the estimated results as initial constraints during the inversion, is more stable. Tests on synthetic data show that fracture weaknesses parameters are still estimated reasonably with moderate noise. A test on real data shows that the estimated results are in good agreement with the drilling.

Keywords: rock physics, fractures, weaknesses, AVAZ, seismic inversion

(Some figures may appear in colour only in the online journal)

1. Introduction

Fractures are the most abundant visible structural feature in the Earth's crust and they are probably more common than we think (Liu and Martinez 2012). In general, the presence of fractures will cause seismic waves to behave differently in different directions. On the other hand, fractures may increase the porosity of the rock, and the flow of hydrocarbons and water. Hence, fractured media have been a hot topic in many disciplines, such as seismic exploration and ground water extraction. Fracture characterization is an important part of reservoir development for carbonate rock reservoirs and unconventional resources (shale gas, tight sand reservoirs, etc).

Recently, rock physics has proved to be a useful tool in reservoir exploration (Chen *et al* 2014). The rock physics effective model can build the bridge between fractured reservoirs parameters and seismic response (Avseth *et al* 2005). In this paper, we aim to build an improved fractured anisotropic rock physics effective model to estimate P-wave velocity, S-wave velocity and fracture weaknesses from the well-logging data. Two very popular rock physics models are used for the derivation of fracture weaknesses. One is Hudson's model for cracked media, which assumes there are thin, penny-shaped ellipsoidal cracks or inclusions in an elastic solid (Hudson 1980). The other is linear slip deformation (LSD) theory for fractured media (Schoenberg and Douma 1988, Schoenberg and Muirt 1989, Schoenberg and Protazio 1992, Schoenberg

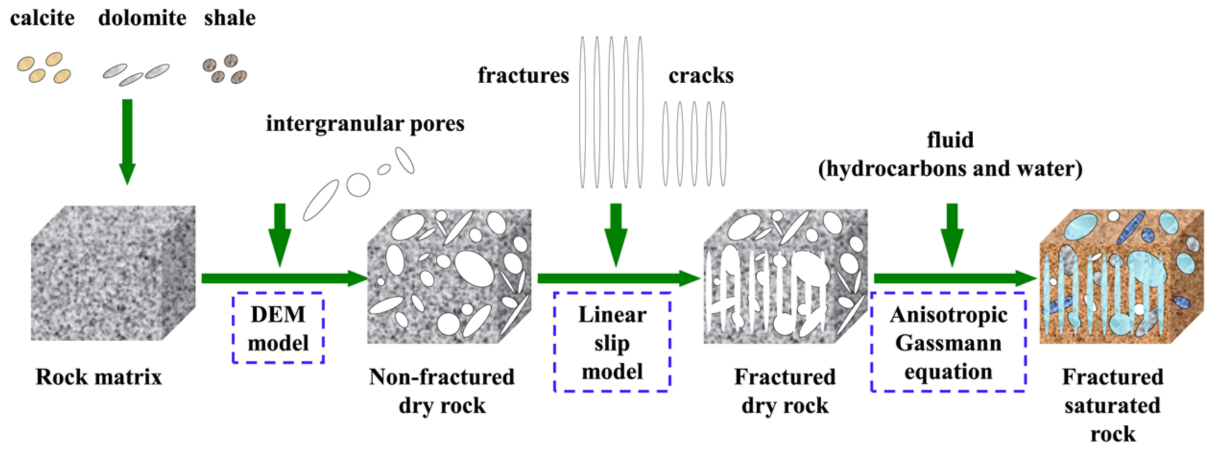

Figure 1. Improved fractured carbonate rock physics model.

and Sayers 1995). For simplification, we further assume the medium is HTI and the noninteractive, vertical fractures contain either water or gas. With these assumptions, fracture weaknesses may be estimated from the well-logging data by using our effective model.

One proven method to predict fractures is the AVAZ inversion method (Gray and Head 2000). Rüger (1997, 1998) Rüger and Tsvankin (1997) derived a linearized approximation to the Zoeppritz equation for HTI anisotropy. Based on this equation, azimuthal seismic gathers are used to estimate the elastic and anisotropic parameters (Mallick *et al* 1998). With the purpose of high-resolution fracture characterization, a new reconstruction of the layer anisotropic elastic parameters was proposed (Bachrach *et al* 2009). Studies show that seismic reflection amplitudes are different when the fractures are filled with different types of fluid (Nuet *et al* 2007, Sil *et al* 2010). That makes it possible to use the AVAZ inversion method to predict the type of fracture fluid (Shaw and Sen 2006).

In this paper, we first provide the process to build the improved fractured anisotropic rock physics effective model. Using this model, we estimate velocities and fracture weaknesses. The fracture weaknesses estimated results may help describe the fracture locations. We also derive a new equation for expressing reflection coefficients of HTI media with fracture weaknesses. Further, we propose a feasible method to estimate fracture weaknesses parameters based on AVAZ inversion. In addition, the influence of noise on seismic inversion is discussed. Tests on synthetic and real data show that the estimation is credible.

2. Theory

2.1. Improved fractured anisotropic rock physics effective model

Anisotropy is caused by sub-seismic rock heterogeneous due to the fractures' preferred alignment. When the scales of fractures are smaller than a seismic wavelength, effective medium theory can be used in building improved fractured rock physics model. Figure 1 shows the basic steps of constructing the model. In our study, we select the carbonate rock as the research object. With reference to the Xu–Payne model (Xu and Payne 2009), we propose our improved fractured anisotropic rock physics effective model.

Carbonate rock matrix is mainly composed of calcite and dolomite (Ruiz and Dvorkin 2009). The pore of fractured carbonate rock may be divided into intergranular pores, cracks and fractures (Kumar and Han 2005). Our study focuses on the vertically aligned fractures. We assume the pore fluid is a mixture of hydrocarbons and water.

(a) Average moduli estimation using the Voigt–Reuss–Hill equation (Hill 1952).
(b) Building a non-fractured dry rock model using a DEM model (Mavko *et al* 2009).
(c) Constructing a fractured dry rock model using a linear slip model (Schoenberg and Sayers 1995).
(d) Fluid substitution using the anisotropic formula (Brown and Korringa 1975).
(e) Estimating parameters based on the Thomsen definition (Thomsen 1986).

Compared to rock physics models for conventional reservoirs (Xu and Payne 2009), the current effective model primarily focuses on the modeling of azimuthal anisotropy resulting from vertical fractures. The fracture weaknesses may be calculated directly by using this model, and the location of fractures may be predicted by analyzing the characteristic of fracture weaknesses. Now we will introduce two very important models, a linear slip model for fractured media and a fluid substitution model for anisotropic media, which are used in building the rock physics effective model.

2.2. Linear slip fracture model

The stiffness matrix of fractured rock may be calculated by using the isotropic elastic parameters λ and μ, and fracture weaknesses Δ_N and Δ_T . Δ_N and Δ_T are related to the anisotropy of fractured rock. The elastic matrix of fractured rock is given as:

$$C=\begin{bmatrix} M(1-\Delta_N) & \lambda(1-\Delta_N) & \lambda(1-\Delta_N) & 0 & 0 & 0 \\ \lambda(1-\Delta_N) & M\left(1-\left(\frac{\lambda}{M}\right)^2\Delta_N\right) & \lambda\left(1-\frac{\lambda}{M}\Delta_N\right) & 0 & 0 & 0 \\ \lambda(1-\Delta_N) & \lambda\left(1-\frac{\lambda}{M}\Delta_N\right) & M\left(1-\left(\frac{\lambda}{M}\right)^2\Delta_N\right) & 0 & 0 & 0 \\ 0 & 0 & 0 & \mu & 0 & 0 \\ 0 & 0 & 0 & 0 & \mu(1-\Delta_T) & 0 \\ 0 & 0 & 0 & 0 & 0 & \mu(1-\Delta_T) \end{bmatrix} \tag{1}$$

where $M=\lambda+2\mu$.

Bakulin *et al* (2000) made a comparison of Hudson's model and linear slip models. Δ_N and Δ_T may be calculated easily combined with Hudson's model

$$\begin{aligned} \Delta_{\mathrm{N}} &= \frac{4e}{3g(1-g)\left[1+\frac{1}{\pi(1-g)}\left(\frac{k'+4/3\mu'}{\mu\alpha}\right)\right]} \\ \Delta_{\mathrm{T}} &= \frac{16e}{3(3-2g)\left[1+\frac{4}{\pi(3-2g)}\left(\frac{\mu'}{\mu\alpha}\right)\right]} \end{aligned} \tag{2}$$

where $g=\mu/(\lambda+2\mu)$. e is fracture density, and α is aperture. k' and μ' are parameters of fillings in fractures.

Combined with a linear slip model, we propose a new expression for the anisotropic parameters

$$\begin{aligned} \delta^{(V)} &= \frac{-2g\left[(1-2g)\Delta_{\mathrm{N}}+\Delta_{\mathrm{T}}\right]\left[1-(1-2g)\Delta_{\mathrm{N}}\right]}{\left[1-\Delta_{\mathrm{N}}(1-2g)^2\right]\left[1+\frac{g\Delta_{\mathrm{T}}-\Delta_{\mathrm{N}}(1-2g)^2}{1-g}\right]} \\ \varepsilon^{(V)} &= \frac{-2g(1-g)\Delta_{\mathrm{N}}}{1-(1-2g)^2\Delta_{\mathrm{N}}} \\ \gamma &= \frac{\Delta_{\mathrm{T}}}{2}. \end{aligned} \tag{3}$$

In the study, we use a linear slip model with the assumption of $k'=0$ and $\mu'=0$ to build a fractured dry rock model.

2.3. Fluid substitution in anisotropic media

Brown and Korringa (1975) studied fluid substitution as seen in equation (4) for the case where the rock is anisotropic

$$c_{ijkl}^{\mathrm{sat}}=c_{ijkl}^{\mathrm{dry}}+\frac{\left(K_0\delta_{ij}-c_{ijaa}^{\mathrm{dry}}/3\right)\left(K_0\delta_{kl}-c_{bbkl}^{\mathrm{dry}}/3\right)}{(K_0/K_{\mathrm{fl}})\phi(K_0-K_{\mathrm{fl}})+\left(K_0-c_{ccdd}^{\mathrm{dry}}/9\right)} \tag{4}$$

where c_{ijkl}^{dry} is the effective elastic stiffness element of dry rock, c_{ijkl}^{sat} is the effective elastic stiffness element of rock saturated with pore fluid, K_0 is the mineral bulk modulus, K_{fl} is the fluid bulk modulus, and ϕ is porosity.

In our steps of building a rock physics effective model, we use equation (4) to calculate the stiffness of fractured saturated rock.

2.4. Reflection coefficient approximate formula containing fracture weaknesses

Rüger (1997, 1998) Rüger and Tsvankin (1997) proposed the PP wave reflection coefficient for HTI media:

$$\begin{aligned} R_{\mathrm{pp}}(\theta,\phi) &= \frac{1}{2}\left(\frac{\Delta\rho}{\bar{\rho}}+\frac{\Delta V_{\mathrm{p}}}{\bar{V}_{\mathrm{p}}}\right) \\ &+\frac{1}{2}\left\{\frac{\Delta V_{\mathrm{p}}}{\bar{V}_{\mathrm{p}}}-\left(2\frac{\bar{V}_{\mathrm{s}}}{\bar{V}_{\mathrm{p}}}\right)^2\left(\frac{\Delta\rho}{\bar{\rho}}+\frac{2\Delta V_{\mathrm{s}}}{\bar{V}_{\mathrm{s}}}\right)\right. \\ &\left.+\left[\Delta\delta^{(V)}+2\left(2\frac{\bar{V}_{\mathrm{s}}}{\bar{V}_{\mathrm{p}}}\right)^2\Delta\gamma\right]\cos^2\phi\right\}\sin^2\theta \\ &+\frac{1}{2}\left\{\frac{\Delta V_{\mathrm{p}}}{\bar{V}_{\mathrm{p}}}+\Delta\varepsilon^{(V)}\cos^4\phi+\Delta\delta^{(V)}\sin^2\phi\cos^2\phi\right\}\sin^2\theta\tan^2\theta \end{aligned} \tag{5}$$

where θ is the incidence angle, and ϕ is the azimuth angle. V_{p}, V_{s}, and ρ are P-wave velocity, S-wave velocity and density, respectively.

A new equation that contains fracture weaknesses is derived at the small incident angle

$$\begin{aligned} R_{\mathrm{pp}}(\theta,\phi) &= \sec^2\theta R_{\mathrm{p}}-8g\sin^2\theta R_{\mathrm{s}}-(g\cos^2\phi\sin^2\theta) \\ &\quad(1-2g)R_{\Delta_{\mathrm{N}}}+(g\cos^2\phi\sin^2\theta)R_{\Delta_{\mathrm{T}}} \end{aligned} \tag{6}$$

where $R_{\mathrm{p}}=\frac{1}{2}\left(\Delta V_{\mathrm{p}}/\bar{V}_{\mathrm{p}}+\Delta\rho/\bar{\rho}\right)$, $R_{\mathrm{s}}=\frac{1}{2}\left(\Delta V_{\mathrm{s}}/\bar{V}_{\mathrm{s}}+\Delta\rho/\bar{\rho}\right)$, $R_{\Delta_{\mathrm{N}}}=\Delta_{\mathrm{N2}}-\Delta_{\mathrm{N1}}$, $R_{\Delta_{\mathrm{T}}}=\Delta_{\mathrm{T2}}-\Delta_{\mathrm{T1}}$. Δ_{N1}, Δ_{N2}, Δ_{T1} and Δ_{T2} are the weaknesses of layers.

On the assumption that the reflection coefficient is for an isotropic half space over an anisotropic half space, equation (6) becomes:

$$\begin{aligned} R_{\mathrm{pp}}(\theta,\phi) &= \sec^2\theta\, R_{\mathrm{p}}-8g\sin^2\theta R_{\mathrm{s}}-(g\cos^2\phi\sin^2\theta)(1-2g)\Delta_{\mathrm{N}} \\ &\quad+(g\cos^2\phi\sin^2\theta)\Delta_{\mathrm{T}}. \end{aligned} \tag{7}$$

The equation is an effective link between seismic reflection characteristics and fractured rock properties.

2.5. AVAZ inversion for fracture weaknesses

Equation (7) shows that fracture weaknesses may be predicted by using seismic inversion. For m offsets and n azimuthal angles, it may be written as:

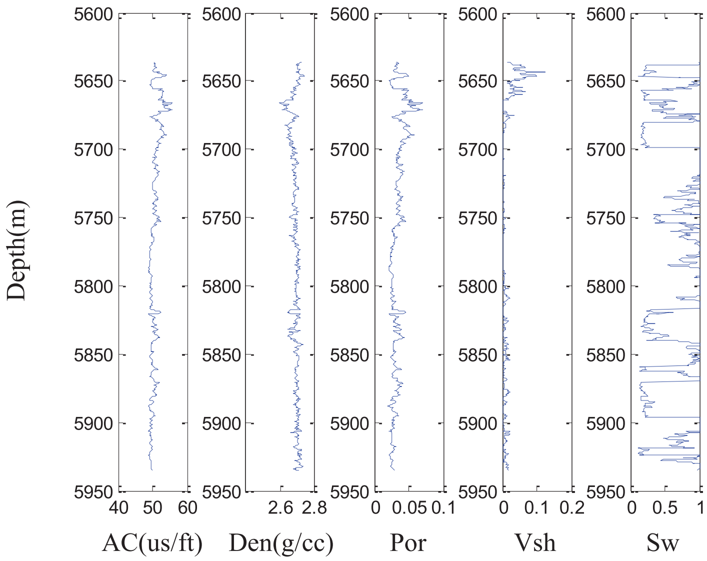

Figure 2. The results of well-logging interpretation.

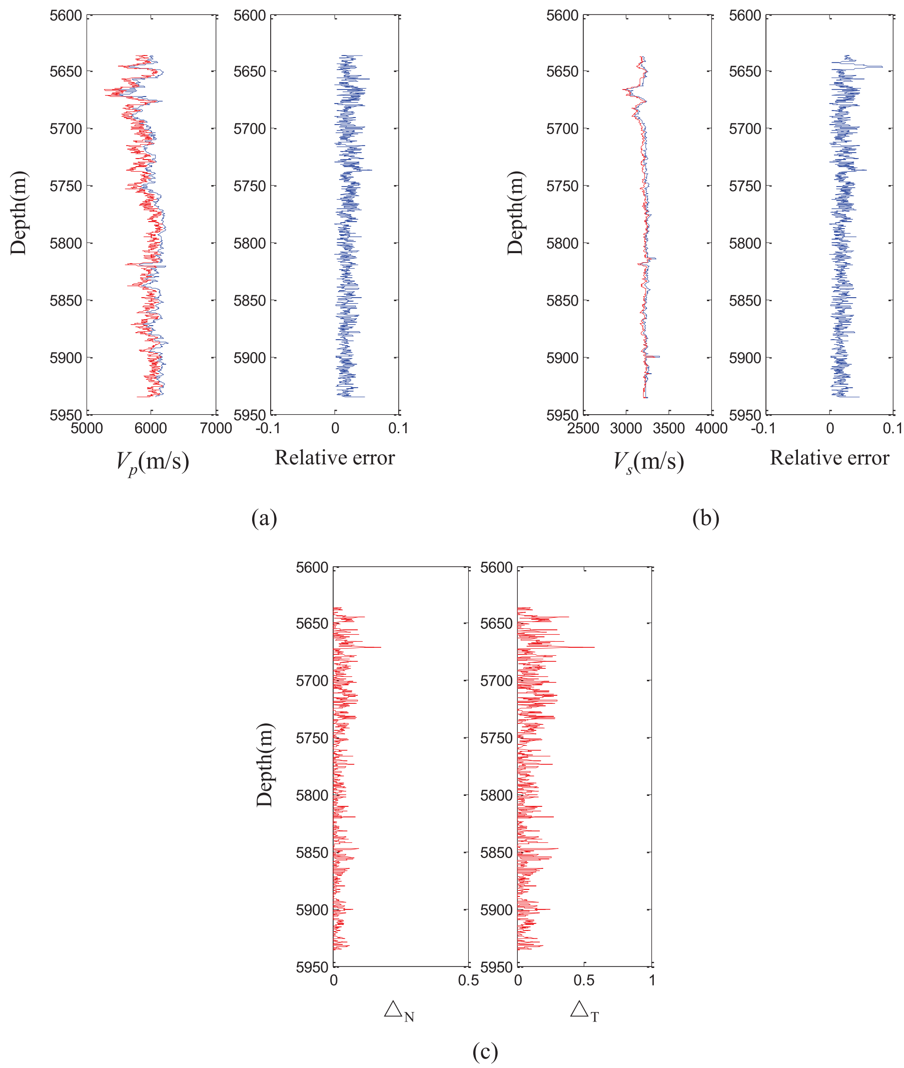

Figure 3. The comparison between the estimated results and true values. (*a*) P-wave velocity estimated result (red line) and true value (blue line). (*b*) S-wave velocity estimated result (red line) and true value (blue line). (*c*) Fracture weaknesses estimated results.

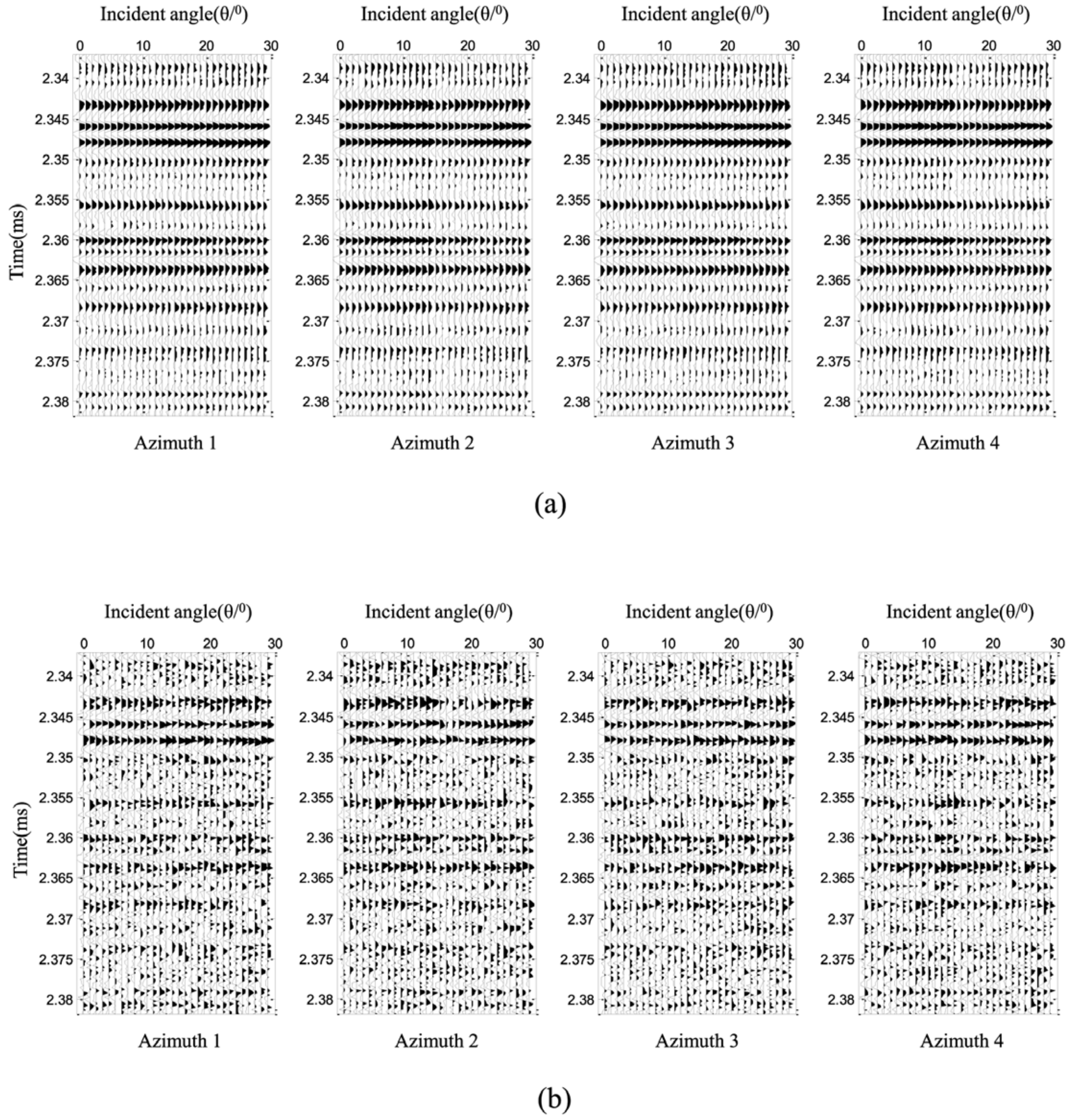

Figure 4. Synthetic profiles with different S/N ratio.

$$\begin{bmatrix} R_{pp}(\theta_1,\phi_1) \\ R_{pp}(\theta_2,\phi_2) \\ \vdots \\ R_{pp}(\theta_m,\phi_n) \end{bmatrix} = \begin{bmatrix} \sec^2\theta_1 & -8g\sin^2\theta_1 & -\left(g\cos^2\phi_1\sin^2\theta_1\right)(1-2g) & g\cos^2\phi_1\sin^2\theta_1 \\ \sec^2\theta_2 & -8g\sin^2\theta_2 & -\left(g\cos^2\phi_2\sin^2\theta_2\right)(1-2g) & g\cos^2\phi_2\sin^2\theta_2 \\ \vdots & \vdots & \vdots & \vdots \\ \sec^2\theta_m & -8g\sin^2\theta_m & -\left(g\cos^2\phi_n\sin^2\theta_m\right)(1-2g) & g\cos^2\phi_n\sin^2\theta_m \end{bmatrix} \begin{bmatrix} R_p \\ R_s \\ \Delta_N \\ \Delta_T \end{bmatrix}. \quad (8)$$

In order to obtain R_p, R_s, Δ_N, and Δ_T, equation (8) is simplified to

$$d = GX \quad (9)$$

where

$$d = \begin{bmatrix} R_{pp}(\theta_1,\phi_1) \\ R_{pp}(\theta_2,\phi_2) \\ \vdots \\ R_{pp}(\theta_m,\phi_n) \end{bmatrix}, G = \begin{bmatrix} \sec^2\theta_1 & -8g\sin^2\theta_1 & -\left(g\cos^2\phi_1\sin^2\theta_1\right)(1-2g) & g\cos^2\phi_1\sin^2\theta_1 \\ \sec^2\theta_2 & -8g\sin^2\theta_2 & -\left(g\cos^2\phi_2\sin^2\theta_2\right)(1-2g) & g\cos^2\phi_2\sin^2\theta_2 \\ \vdots & \vdots & \vdots & \vdots \\ \sec^2\theta_m & -8g\sin^2\theta_m & -\left(g\cos^2\phi_n\sin^2\theta_m\right)(1-2g) & g\cos^2\phi_n\sin^2\theta_m \end{bmatrix}, X = \begin{bmatrix} R_p \\ R_s \\ \Delta_N \\ \Delta_T \end{bmatrix}.$$

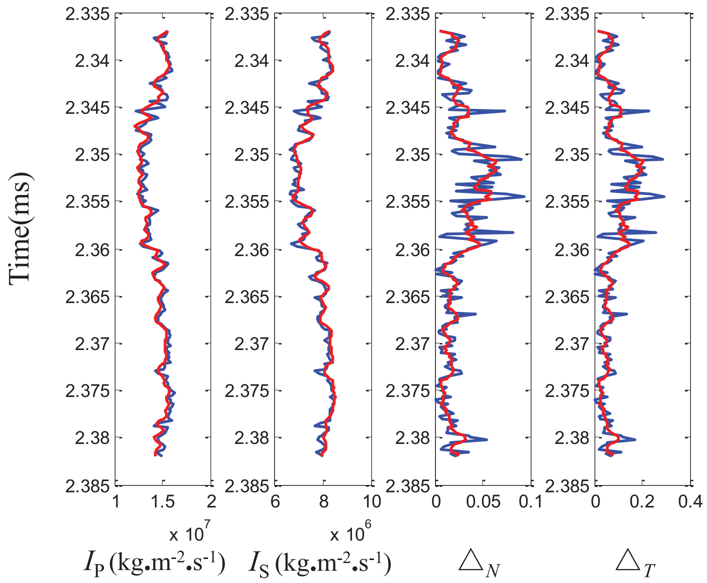

(a)

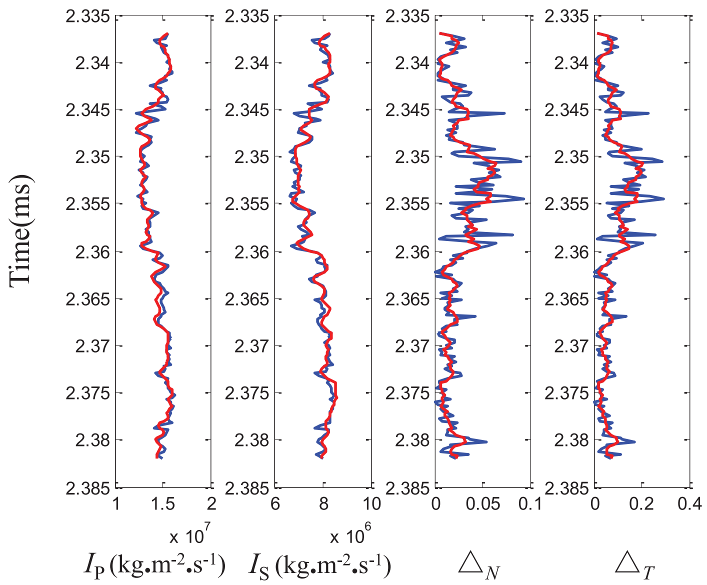

(b)

Figure 5. Model inversion results with different noise.

We add noise, N, to equation (9) and it becomes:

$$d + N = GX. \tag{10}$$

Using the damped least squares method, we get:

$$X = \text{mod}\_X + [G^{\mathrm{T}}G + \sigma I]^{-1}\, G^{\mathrm{T}}(d - G * \text{mod}\_X) \tag{11}$$

where mod $\_X$ is the parameter of the initial model, which may be obtained using our rock physics effective model. G^{T} is the transpose of matrix G. σ is the damping factor. I is an identity matrix. The choice of damping factor depends mainly on experiments. In the extreme, when there is no noise, σ is zero.

3. Example

3.1. Estimation of parameters using the improved fractured rock physics effective model

Well A from a fractured carbonate rock work area is used to validate our rock physics effective model. Figure 2 shows the results of well-logging interpretation: acoustic slowness curve (AC), density curve (Den), porosity curve (Por), clay content curves (Vsh) and water saturation curve (Sw). Figure 3(*a*) is the P-wave velocity comparison between the estimated result and the true value. Figure 3(*b*) is the S-wave velocity

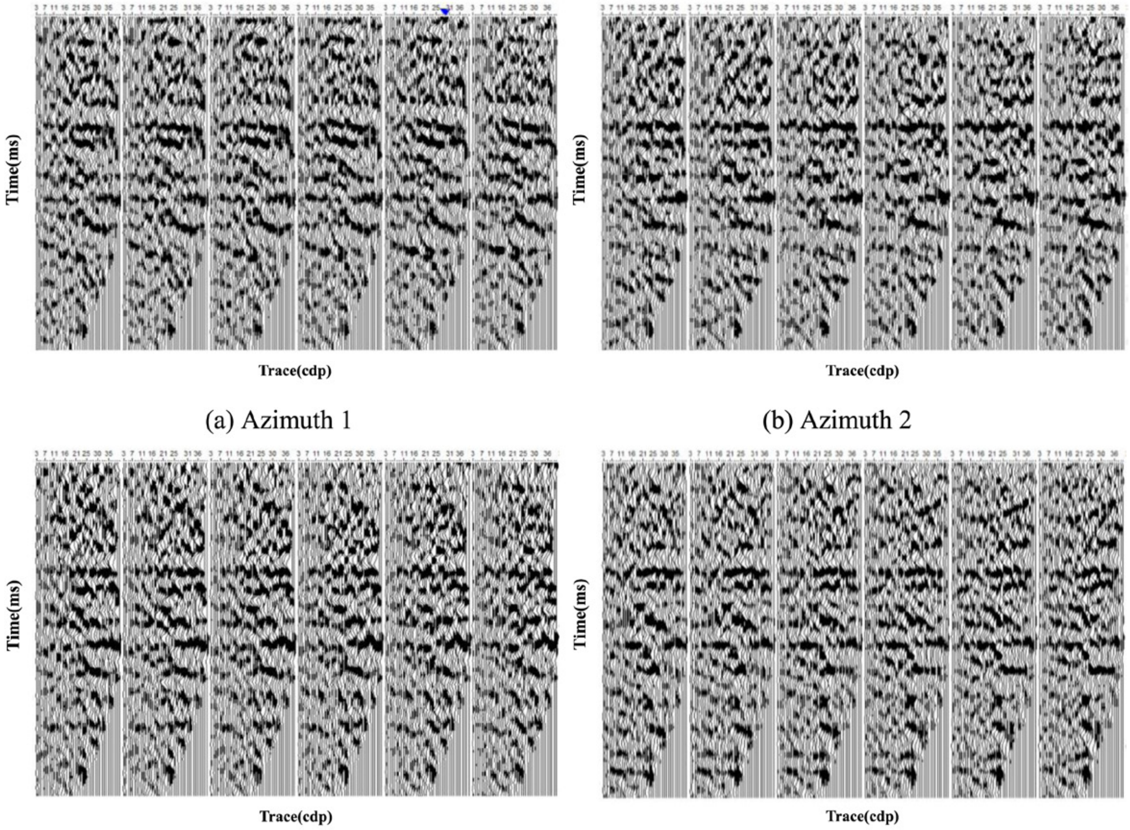

(a) Azimuth 1 (b) Azimuth 2

(c) Azimuth 3 (d) Azimuth 4

Figure 6. Azimuthal angle pre-stack seismic profiles.

comparison between the estimated result and the true value. Figure 3(*c*) is the fracture weaknesses estimated results.

3.2. Synthetic test

We test the AVAZ inversion method on synthetic seismic profiles from real well B. To test the stability of the inversion method, we add random noise to the synthetic traces. The signal-to-noise (S/N) ratios are 4 and 1, respectively (figure 4). Figure 5 shows original (in blue) and inverted (in red) P-wave impedance I_p, S-wave impedance I_s, the normal weakness Δ_N and the tangential weakness Δ_T of well B with different S/N ratios. It is easy to demonstrate that P-wave impedance, S-wave impedance and fracture weaknesses are estimated well even when the S/N ratio is 1.

3.3. Real data

Real data is used to validate the application of the AVAZ inversion method. True amplitude processing has been implemented before the inversion.

The seismic data was processed using a contractor and the processing sequence was defined to ensure that the final pre-stack amplitudes should image the reflection strength of the subsurface interfaces as correctly as possible. We assume that wave mode conversions and interbed multiples effects may be neglected after processing.

Four partial angle stack seismic profiles are shown in figure 6. The maximum incident angle is around 35°. The estimated P-wave impedance, S-wave impedance and fracture weaknesses are displayed in figure 7. Figure 7 shows the target reservoir is around 4070 ms (CDP 1400). From the inverted results, we may see that P- and S-wave impedances show low value, and the normal and tangential weaknesses show high value. This result is consistent with the drilling and rock physics analysis.

Schoenberg and Sayers (1995) proposed that K_N / K_T might be applied to indicate the fracture fluid. The definition of K_N / K_T is shown as follows:

$$\frac{K_N}{K_T} = \frac{\frac{\Delta_N}{(\lambda + 2\mu)(1 - \Delta_N)}}{\frac{\Delta_T}{\mu(1 - \Delta_T)}} = g\frac{\Delta_N\,(1 - \Delta_T)}{\Delta_T\,(1 - \Delta_N)} \quad (12)$$

Using equation (12), we may calculate fracture fluid factor, K_N / K_T, after the estimation of elastic parameters and fracture weaknesses (figure 8).

4. Conclusions

In this paper, an improved fractured rock physics model is built for estimating P-wave velocity, S-wave velocity, the normal weakness and the tangential weakness. A new reflection coefficient approximate equation that contains

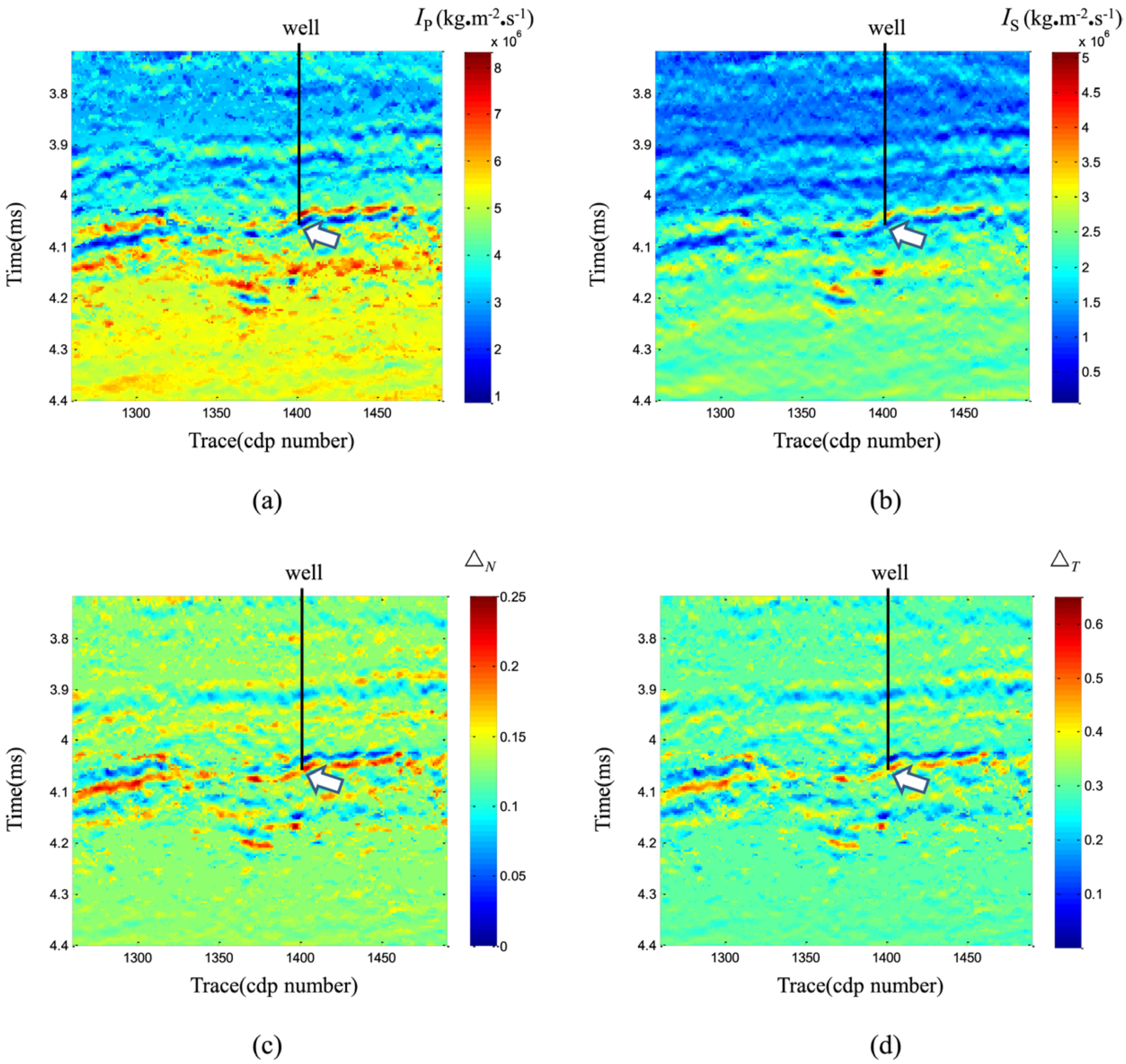

Figure 7. Elastic and fracture weaknesses estimated results. (*a*) P-wave impedance estimated results. (*b*) S-wave impedance estimated results. (*c*) The normal weakness estimated results. (*d*) The tangential weakness estimated results.

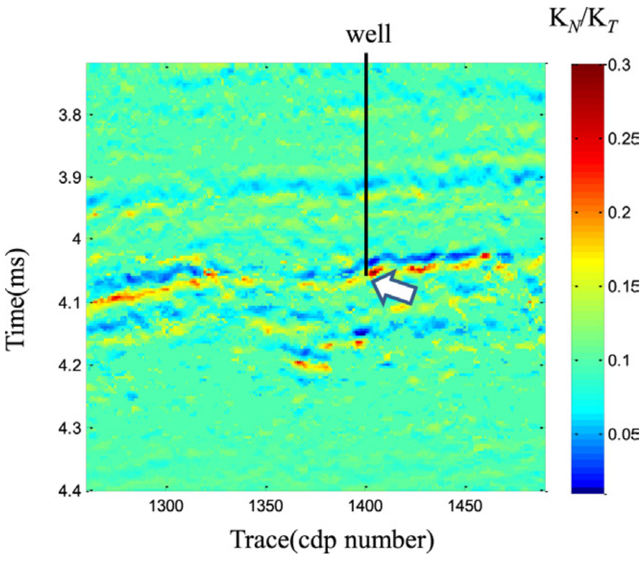

Figure 8. Fracture fluid factor estimated results.

fracture weaknesses is derived for HTI media. One new approach, which is based on AVAZ inversion for P-wave impedance, S-wave impedance, the normal weakness and the tangential weakness directly, is proposed. Well A is used to verify the improved fractured rock physics effective model. Synthetic and real data from fractured reservoirs are used to validate the AVAZ inversion method. The results estimated by using the rock physics effective model may provide an initial constraint for AVAZ inversion. The inverted results, which well match the logging data, show us that the AVAZ inversion method is stable and reasonable, and it may help reduce the uncertainty for the estimation of fracture weaknesses.

It is well known that fluid identification in fractures is very important. Thus, an effective fluid identification factor is necessary. Hence, the next study is to introduce a useful fluid identification factor. In addition, we will also find an effective method to estimate the fluid identification factor in fractured reservoirs.

Acknowledgments

This work is supported by the National Basic Research Program of China (973 Program, 2013CB228604, 2014CB239201), the National Oil and Gas Major Projects of China (2011ZX05014 -001-010HZ), CNPC Innovation Foundation (2011D-5006-0301), the Fundamental Research Funds for the Central Universities in China (14CX06015A) and SINOPEC Key Laboratory of Geophysics.

References

Avseth P, Mukerji T and Mavko G 2005 *Quantitative Seismic Interpretation* (Cambridge: Cambridge University Press)
Bachrach R, Sengupta M and Salama A 2009 Reconstruction of the layer anisotropic elastic parameter and high resolution fracture characterization from P-wave data: a case study using seismic inversion and Bayesian rock physics parameter estimation *Geophys. Prospect.* **57** 253–62
Bakulin A, Grechka V and Tsvankin I 2000 Estimation of fracture parameters from reflection seismic data—part I HTI model due to a single fracture set *Geophysics* **65** 1788–802
Brown R and Korringa J 1975 On the dependence of the elastic properties of a porous rock on the compressibility of the pore fluid *Geophysics* **40** 608–16
Chen H Z, Zhang G Z and Chen J J 2014 Fracture filling fluids identification using azimuthally elastic impedance based on rock physics *J. Appl. Geophys.* **110** 98–105
Gray D and Head K 2000 Fracture detection in Manderson field: a 3D AVAZ case history *Leading Edge* **19** 1214–21
Hill R 1952 The elastic behavior of crystalline aggregate *Proc. Phys. Soc.* **65** 349–54
Hudson J A 1980 Overall properties of a crack solid *Math. Proc. Camb. Phil. Soc.* **88** 371–84
Kumar M and Han D H 2005 Pore shape effect on elastic properties of carbonate rocks *75th SEG Meeting (Houston, TX)* expanded abstracts pp 1477–81
Liu E and Martinez A 2012 *Seismic Fracture Characterization* (Netherlands: EAGE Publication)
Mallick S, Craft K L and Meister L J 1998 Determination of the principal directions of azimuthal anisotropy from P-wave seismic data *Geophysics* **63** 692–706
Mavko G, Mukerji T and Dvorkin J 2009 *The Rock Physics Handbook* 2nd edn (Cambridge: Cambridge University Press)
Nuet J V, Shaw R K and Sen M K 2007 Estimation of the fluid indicator from azimuthal AVO gradient variations at a fractured reservoir *77th SEG Meeting (San Antonio, TX)* expanded abstracts pp 239–43
Rüger A 1997 P-wave reflection coefficients for transversely isotropic models with vertical and horizontal axis of symmetry *Geophysics* **62** 713–22
Rüger A 1998 Variation of P-wave reflectivity with offset and azimuth in anisotropic media *Geophysics* **63** 935–47
Rüger A and Tsvankin I 1997 Using AVO for fracture detection: Analytic basis and practical solutions *Leading Edge* **16** 1429–34
Ruiz F and Dvorkin J 2009 Sediment with porous grains: rock physics model and application to marine carbonate and opal *Geophysics* **74** E1–15
Schoenberg M and Douma J 1988 Elastic wave propagation in media with parallel fractures and aligned cracks *Geophys. Prospect.* **36** 571–90
Schoenberg M and Muirt F 1989 A calculus for finely layered anisotropic media *Geophysics* **54** 581–9
Schoenberg M and Protazio J 1992 'Zoeppritz' rationalized and generalized to anisotropy *J. Seis Expl.* **1** 125–44
Schoenberg M and Sayers C M 1995 Seismic anisotropy of fractured rock *Geophysics* **60** 204–11
Shaw R K and Sen M K 2006 Use of AVOA data to estimate fluid indicator in a vertically fractured medium *Geophysics* **71** C15–24
Sil S, Sen M K and Gurevich B 2010 Sensitivity analysis of fluid substitution in a porous medium with aligned fractures *80th SEG Meeting (Denver, CO)* expanded abstracts pp 202–6
Thomsen L 1986 Weak elastic anisotropy *Geophysics* **51** 1954–66
Xu S Y and Payne M A 2009 Modeling elastic properties in carbonate rocks *Leading Edge* **28** 66–74